Postprint of: Ferenc T., Multiparameter sensitivity analysis of a GFRP composite footbridge of a sandwich structure and U-shaped cross-section, Composite Structures, Vol. 253 (2020), 112793, DOI: 10.1016/j.compstruct.2020.112793

Multiparameter sensitivity analysis of a GFRP composite footbridge of a sandwich structure and U-shaped cross-section

Tomasz Ferenc

Gdansk University of Technology, Faculty of Civil and Environmental Engineering

ABSTRACT

The paper deals with multiparameter sensitivity analysis of a composite footbridge. A shell-like structure is 14.5 m long shows U-shaped cross-section and inner service dimensions 1.3 x 2.5 m. Glass fiber reinforced polymer GFRP laminate constitutes faces of a sandwich structure while PET foam received from recycled bottle builts a core. The structure was divided into 285 independent areas where the thickness of laminates and stiffness modulus of PET foam were established as design variables. The impact of their variation on variation of state variables was investigated, vertical displacement of structure, longitudinal strain in handrail and transverse strain in deck were addressed here. Sensitivity vector was computed by a semi-analytical method and, subsequently, expressed in a matrix form and next presented graphically in the form of sensitivity areas. The conducted sensitivity analysis exhibits areas that can be strengthened in order to minimize vertical displacement, longitudinal strain in handrail and transverse strain deck, determining the areas where parameters can be reduced without increasing the value of state variables. The obtained results are bound to support the structural design process or to improve the performance of existing structures.

Keywords: Sensitivity analysis, composite footbridge, sandwich structure, GFRP laminate, PET foam, semi-analytical method

1. Introduction

The design of all types of engineering structures is a complicated and lengthy process. It often involves creating a complex mathematical model representing the real structure. Afterwards, many aspects of its behavior have to be studied, the possilbe problems have to be solved, involving statics, dynamics or buckling. Sensitivity analysis is a useful tool in this process by means of the information on the impact of chosen parameters describing the model on the structural response [1] [2]. The obtained results can also be applied to solve the optimization problems [3] [4] [5] [6].

Two methods of sensitivity analysis can be distinguished: continuum (or variational) method and discrete (or implicite differentiation) method. In the course of the continuum method a continuous mathematical model represents the real structure [7]. However, due to complexity and difficulties in solving mathematical equations, and the widespread use of Finite Element Method (FEM) to represent behavior of real structures, the discrete sensitivity method becomes more popular [8]. Moreover, the discrete method approaches can be divided into the analytical method (AM) [9] [10] [11] [12] [13] [14] and the semi-analytical method (SAM) [15] [16] [17] [18] [19] [20]. Generally, in order to conduct sensitivity analysis discrete methods require the derivatives of a stiffness matrix or a mass matrix with respect to chosen design variables. The AM method is based on analytical computation of that derivatives. However, in many cases, it is difficult and sometimes impossible due to lack of access to internal source of software, e.g. implicit character of stiffness or mass matrix. Thus the SAM method can be used as a response for this inconvenience where derivatives can be approximated by means of a finite difference method. On the other hand, approximation always results in an error, and therefore the improved semi-analytical method is studied [17] [18] [19] [20].

Nowadays composites structures are widespread on aviation or maritime industry, but they become more popular in civil engineering, especially in bridge structures [21] [22]. Fiber

reinforced polymer (FRP) composites meet the requirements as their strength is increased with minimized mass, comparing to traditional materials like steel [23]. Moreover, the FRP composite exhibits high corrosion resistance, low thermal expansion and especially the ability of forming almost unrestricted shape [24] [25]. Thus, reinforcement can be individually arranged in order to increase structural capacity under applied loading. Therefore, the design of structures made of composite material is a very complex problem.

Until recently, structural elements made of FRP composites applied in bridges were mainly manufactured in pultrusion process and applied in structures of truss models. However, the manufacturing technology of composite structures improves every year, providing new possibilities for shape forming and cost reduction. The recent years increased the application of large scale structural elements in bridges, moreover, entire structures are designed to be fully made from composites. To take full advantage of the properties of FRP elements in road bridges, traditional steel girders are replaced by composite members [26] [27] [28]. Similarly, cables traditionally made of high-strength steel are substituted by FRP composites [29] [30]. Besides, also time-honored concrete deck is bound to be replaced by composite panels to minimize mass of the structure [31] [32]. There exist structures, mainly footbridges, made of composite materials alone [33] [34] [35]. Additionally, theoretical studies are widely conducted in order to design new structure with the use of FRP [36] [37] [38].

The aim of the presented research is to present the possibility of applying sensitivity analysis for a novel composite footbridge, which is a sandwich structure made of GFRP laminate and PET foam. The innovative structure with theoretical length of 14 m was studied in the paper in order to improve its behavior under the serviceable loading. The objective of the paper is to find areas of the structure with the highest or the lowest sensitivity that affects the structural response: vertical displacement, longitudinal and transverse strain in chosen points in the mid-span length.

2. Description of the footbridge

The structure considered in the paper was designed, manufactured and studied as a part of the grant conducted by Gdansk University of Technology, Military University of Technology in Warsaw and private company ROMA Sp. z o.o. throughout the years 2013-2015 [33]. Several numerical, experimental and technological investigations were carried out in the project framework. Standard specimens were tested in order to determine material parameters [39] [40]. Moreover, experiments performed on specimens with greater dimensions i.e. sandwich beams [41] or a footbridge segment of a 3 m length [42] [43] [44] [45] allow to validate numerical models applied to design the target structure. Finally, the footbridge was manufactured by the infusion process and investigated in Gdansk University of Technology campus (Fig. 1a). Short and long-term static tests and dynamic experiments have been performed [46] [47]. Upon positive evaluation, the footbridge was installed over Radunia River near Gdańsk, Poland to currently serve the pedestrians and cyclists (Fig. 1b). Nevertheless, some further analysis is conducted up till now, i.e. parametric optimization or sensitivity analysis in order to make the structure more competitive in the global market [48] [49].

(a) (b)

Fig. 1. The footbridge (a) during examination in Gdansk University of Technology campus [46], (b) installed for public traffic over Radunia River near Gdańsk, Poland

The footbridge was fully made of composite materials as a shell-like structure, manufactured as a single element in a single technological process. The cross-section is constant along the entire structural length (Fig. 2) and is U-shaped with service width of 2.5 m and depth of walls 1.3 m due to requirements of Polish and European law for pedestrian and cyclic traffic.

The total length of the performed structure is 14.5 m, while the theoretical length is 14 m. Moreover, the structure is designed to be manufactured with the length up to 16 m.

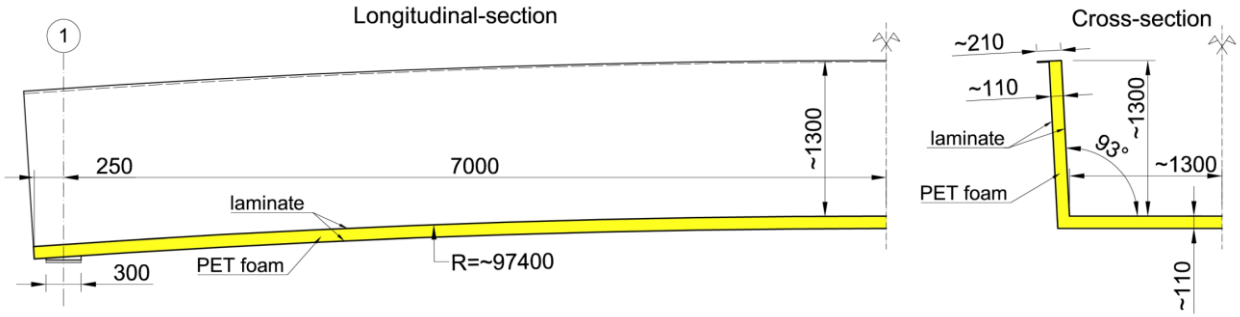

Fig. 2. Dimensions of the footbridge

The footbridge is a sandwich structure with glass fiber reinforced polymer GFRP laminate as faces and PET foam as a core. A six-layered laminate is constituted by vinylester polymer resin reinforced by glass stitched two-directional fabrics BAT and GBX with fiber orientation (0/90) and (+45/-45) respectively. Both, with the same density and amount of fibers in two directions, are regarded as a single ply whose thickness is $0.663 \cdot 10^{-3}$ m. Its material properties were determined after several experiments conducted in Military University of Technology in Warsaw [39]. They are presented in a principal direction of the ply, listed in Table 1.

Table 1. Material parameters of single GFRP ply [39]

Parameter		Value	Unit	Description
E_1	E_2	23.4	[GPa]	longitudinal (1) and transverse (2) elastic moduli
ν_{12}		0.153	[-]	Poisson's ratio
G_{12}		3.52	[GPa]	in-plane shear modulus
G_{13}	G_{23}	1.36	[GPa]	transverse shear moduli
X_t	Y_t	449	[MPa]	longitudinal (1) and transverse (2) strength in tension
X_c	Y_c	336	[MPa]	longitudinal (1) and transverse (2) strength in compression
S		45.2	[MPa]	in-plane shear strength
S_t		34.7	[MPa]	transverse shear strength

The stack sequence of plies is constant through whole structure, it reads [BAT/GBX/BAT_2/GBX/BAT], equivalent to [(0/90)/(+45/-45)/(0/90)/(90/0)/(-45/+45)/(90/0)]. Hence, the laminate is symmetric and six-layered of a total thickness of $3.978 \cdot 10^{-3}$ m assumed as a quasi-isotropic material. Furthermore, PET foam, received from

recycled bottles, shows constant properties along a structure - density equal 100 kg/m^2 and thickness 0.1 m. The material properties of foam follow the manufacturers specification, listed in Table 2.

Table 2. Material parameters of PET foam

Parameter	Value	Unit	Description
E	0.07	[GPa]	elastic modulus
v_{12}	0.4	[-]	Poisson's ratio
R_t	2.7	[MPa]	strength in tension
R_c	1.8	[MPa]	strength in compression

The footbridge is subjected to a surface loading applied on a deck according Eurocode EN 1991. The load value was assumed q_t = 5 kN/m^2. Moreover, the structure was supported on four elastomeric bearings of dimensions 0.30x0.30 m providing a simple support scheme.

The design process of a structure was complex due to the small number of standards, it includes: experimental, numerical and technological investigations. Based on their results and conclusions, the conditions and requirements were outlined for the designed structure. The Ultimate Limit State ULS and Serviceability Limit State SLS are checked according to Eurocode EN 1990: [50]. The ULS focuses on structural safety which leads to control stresses or strains. As the sandwich structure consists of two components, conditions are set individually. Thus the capacity of a laminate is estimated not to exceed the failure index FI = 0.2 according to Tsai-Wu hypothesis [51] [52], to prevent occurrence of micro-cracking in resin [53], while in foam, the extreme stress can reach up to 80% of its strength. On the other hand, the SLS requires that displacements do not exceed a limited value. The maximum displacement were taken after Polish standard PN-S-10052-1982 [54] for plated beam span of steel road bridge which is $v_{\max}$ = L/300 equal to v_{max} = 48.33·10^{-3} m for the analyzed structure.

3. Numerical model of the footbridge

The numerical model of the footbridge was created in FEMAP with NX Nastran environment employing Finite Element Method to assess the structural response under assumed load. As a result of various static and dynamic experimental tests on segment with full-scaled cross-section and the length reduced to 3 m (e.g. [42]), the shell-solid hybrid FEM model was chosen to represent the sandwich structure. Thus the GFRP laminate which constitutes faces is modeled by means of shell four-nodes elements while the PET foam is represented by solid eight-nodes elements. Both models exhibit linear shape functions and full integration. Due to the designed stack sequence of laminate plies, where fibers are orientated in 0, +/-45 and 90 direction, the laminate is considered quasi-isotropic material with properties assumed as follows: elastic moduli E = 23.4 GPa and Poisson's ratio ν = 0.153. However, in the previous analysis (e.g. [48]) other models were considered, assuming the laminate as a single layered shell with orthotropic properties or as a multilayered shell. In the second case, the Equivalent Single Layer ESL theory was applied, here the laminate is represented by a single layered shell of equivalent properties [55]. The three models are compared with the real structural behavior [46]. Values in the mid-span: vertical displacement v_z, longitudinal strain in handrail ε_{x1} and transverse strain in the deck ε_{y2}, the analytical results of the models were compared with the experimental one and listed in Table 3. Modeling the laminate in the form of a single layered shell of isotropic properties simulates behavior of the structure with even higher accuracy than in the case of orthotropic properties or as a six-layer shell by means of ESL theory.

Due to symmetry, only a quarter of the structure has been analyzed (Fig. 3a). The characteristic size of a single finite element was assumed approximately 0.025 m (Fig. 3b). Hence, a total number of elements was equal to 210.207, while a total number of nodes was 178.638. The boundary conditions, the value of pressure acting on a footbridge deck and the bearing dimensions, were assumed as in the previous chapter.

Table 3. Comparison of values obtained from experiment and various models

Model	v_z		ε_{x1}		ε_{y2}	
	value [mm]	error [%]	**value** [μm/m]	error [%]	**value** [μm/m]	error [%]
Experiment [46]	31.4	-	-885	-	345	-
Laminate as a single layered shell with isotropic properties	**34.35**	**9.39%**	**-1048.9**	**18.52%**	**477.9**	**38.52%**
Laminate as a single layered shell with orthotropic properties [48]	37.64	19.87%	-1081.1	22.16%	497.4	44.17%
Laminate as a six-layered shell by means of ESL theory [48]	38.75	23.41%	-1215.0	37.29%	507.9	47.22%

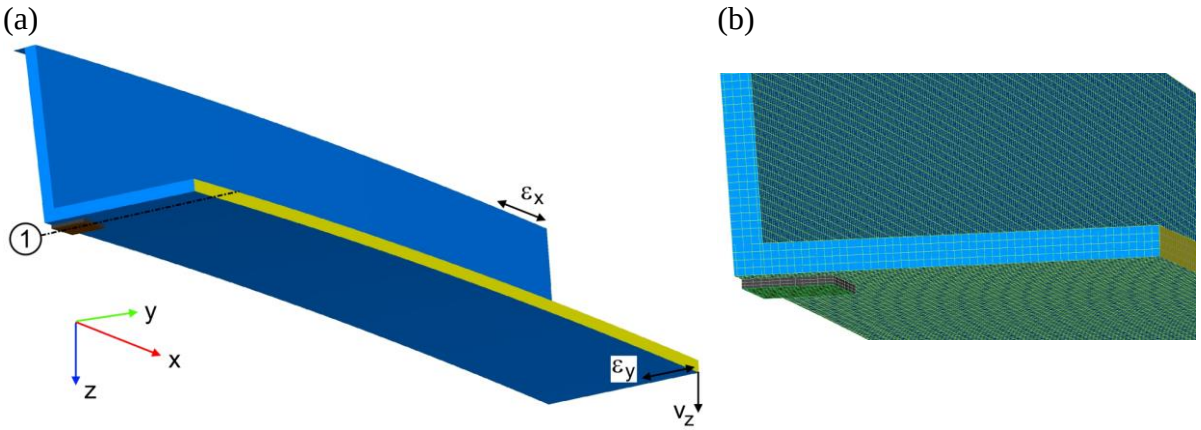

Fig. 3. Numerical model of the footbridge: (a) overall view, (b) FEM mesh size

It is worth mentioning, that laminate can also be modeled in three-dimensional 3D theory with solid elements of various properties along the thickness of laminate [56], or, in the case of reduced thickness of each ply by means of Layerwise LW theory [57] [58]. Although the approaches are more sophisticated, in the scale of the analyzed structure the reduction of multilayered laminate thickness according to ESL theory proves sufficient leading to the decrease of computational time.

4. Sensitivity analysis

Simulation or prediction of real structural behavior is one of the most challenging tasks to complete during design process. Generally, it involves creating the mathematical model

fulfilling all requirements and assumptions. The parameters defining mathematical model can be divided into three groups:

- design variables, b_i, where $i = 1, 2, \ldots, n_1$, stated by the designer directly, i.e. dimensions of cross-section, length of structure or its elements, material parameters, etc.
- model parameters p_j, where $j = 1, 2, \ldots, n_2$, which are fixed, without any impact of the designer, i.e. construction height or span length of bridge determined by the obstacle under the structure, etc.
- state variables S_k, where $k = 1, 2, \ldots, n_3$, structural responses, i. e. cross-sectional forces, stresses, strains, natural frequencies and corresponding mode shapes in dynamics.

In a deterministic approach structural analysis deals with determination of state variables S_k given determined values of design variables b_i and model parameters p_j. In practice, however, the task is inverse. Expecting a certain value or range of state variables S_k, the design variables b_i are selected while model parameters p_j are pre-set. The presented sensitivity analysis discussed in the paper is an inverse problem. Its aims at determining of variations of design variables in the function of variation of state variables, assuming model parameters fixed. Sensitivity analysis is based on the Taylor theorem (e.g. [1]), approximating of differentiable function around a given point by a *k*-th order Taylor polynomial, here the function of a chosen state variable *S* in determined by the initial value of design variables:

$$S(b_0 + \delta b_0) \cong S(b_0) + \delta S(b_0) + \delta^2 S(b_0) + \ldots. \tag{1}$$

The structural response described by the state variable *S*, taking into account only two first components of eq. (1) is a linear approximation of the solution given an initial value of the design variable b_0 (Fig. 4a). On the other hand, considering the following components of eq. (1) the function *S* would be approximated with a higher order function, the approximation error

would decrease (Fig. 4b). However, a linear approximation concept is employed in the paper for two main reasons. The variation of design variables b_i is usually small which means that even their linear approximation is close to the solution. Sensitivity coefficient or sensitivity vectors provide a direct relation of variations of state and design variables.

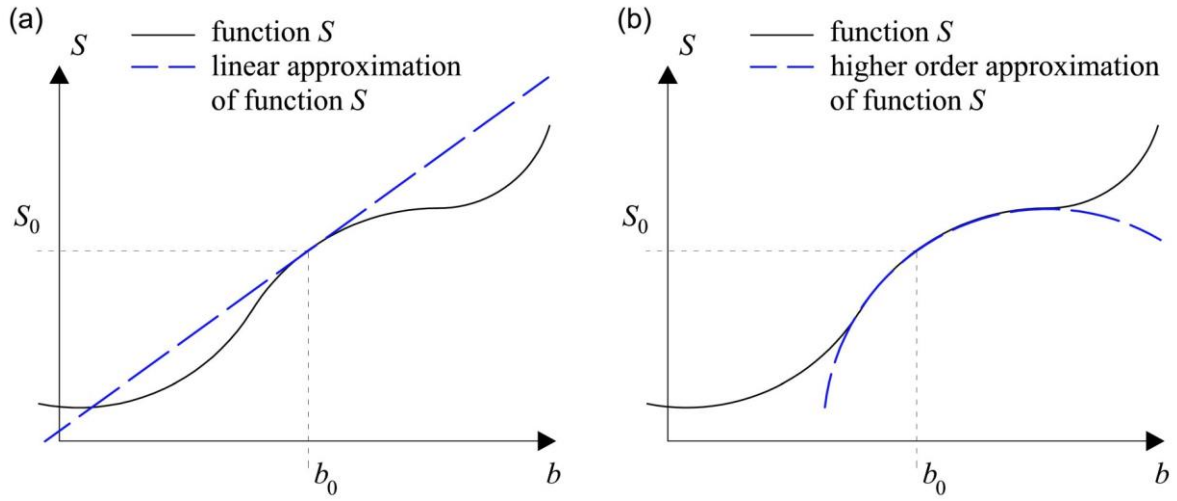

Fig. 4. Approximation concept of a function *S*: (a) linear, (b) higher order

The mathematical model may be a continuous or a discrete one. The first approach is rather theoretical, possible to apply in simple cases only. In the latter case procedure starts with the Finite Element Method, defining geometry and structural response by nodal values generated together with the mesh. Thus more demanding structures may be regarded like the one which is the subject of designers consideration. In this case, the basic FEM equation reads:

$$\mathbf{K}(\mathbf{b})\mathbf{q}(\mathbf{b}) = \mathbf{p}(\mathbf{b}), \tag{2}$$

where $\mathbf{K}(\mathbf{b})$ is a global stiffness matrix, $\mathbf{q}(\mathbf{b})$ is a global displacement vector and $\mathbf{p}(\mathbf{b})$ is a global load vector. All three objects are, generally, functions of vector of design variables $\mathbf{b} = \{b_1, b_2, ..., b_n\}^T$. In a general case, sensitivity of a state variable *S* depends on both design variables $\mathbf{b}$ and displacement vector $\mathbf{q}(\mathbf{b})$, hence $S = S(\mathbf{b}, \mathbf{q}(\mathbf{b}))$. Searching for the relation between state variable *S* and design variables $\mathbf{b}$, variation of state variable δS has to be computed relative to variation of any design variable $\delta\mathbf{b} = \{\delta b_1, \delta b_2, ..., \delta b_n\}^T$. In discrete description, the exact differential equation of function *S* has to be considered:

$$\delta S = \frac{\mathrm{d}S}{\mathrm{d}b_i}\delta b_i = \left(\frac{\partial S}{\partial b_i} + \frac{\partial S}{\partial \mathbf{q}(\mathbf{b})}\frac{\mathrm{d}\mathbf{q}(\mathbf{b})}{\mathrm{d}b_i} \right) \delta b_i \,. \tag{3}$$

Differentiating eq. (2) leads to:

$$\frac{\partial \mathbf{K}(\mathbf{b})}{\partial b_i}\mathbf{q}(\mathbf{b}) + \mathbf{K}(\mathbf{b})\frac{\mathrm{d}\mathbf{q}(\mathbf{b})}{\mathrm{d}b_i} = \frac{\partial \mathbf{p}(\mathbf{b})}{\partial b_i}\,, \tag{4}$$

here, the expression $\frac{\mathrm{d}\mathbf{q}(\mathbf{b})}{\mathrm{d}b_i}$ can be determined from eq. (4) and substituted to eq. (3) which lead to

$$\delta S = \left[\frac{\partial S}{\partial b_i} + \frac{\partial S}{\partial \mathbf{q}(\mathbf{b})}\mathbf{K}^{-1}(\mathbf{b})\left(\frac{\partial \mathbf{p}(\mathbf{b})}{\partial b_i} - \frac{\partial \mathbf{K}(\mathbf{b})}{\partial b_i}\mathbf{q}(\mathbf{b}) \right) \right] \delta b_i = w_{S,i}\delta b_i \,, \tag{5}$$

where $w_{S,i} = \frac{\partial S}{\partial b_i} + \frac{\partial S}{\partial \mathbf{q}(\mathbf{b})}\mathbf{K}^{-1}(\mathbf{b})\left(\frac{\partial \mathbf{p}(\mathbf{b})}{\partial b_i} - \frac{\partial \mathbf{K}(\mathbf{b})}{\partial b_i}\mathbf{q}(\mathbf{b}) \right)$ is a first order sensitivity coefficient of state variable variation δS relative to design variable variation δb_i.

Conducting multiparameter sensitivity analysis, when the state variable is affected by a number of design variables, eq. (5) may be developed as follows:

$$\delta S = \mathbf{w}_S \, \delta \mathbf{b} \,, \tag{6}$$

where $\mathbf{w}_S = \{w_{S,1}, w_{S,2}, ..., w_{S,n}\}$ is a sensitivity vector containing sensitivity coefficients, while $\delta \mathbf{b} = \{\delta b_1, \delta b_2, ..., \delta b_n\}^T$ is a vector of design variable variations.

In order to determine sensitivity coefficients by means of commercial software the eq. (5) may be excluded due to the lack of access to internal source, e.g. implicit character of stiffness or mass matrix. Hence, semi-analytical sensitivity analysis may be conducted in order to find the sensitivity coefficient which can be possibly computed with the use of central difference equation:

$$w_i = \frac{\frac{S(b_0 + \Delta b_i)}{S_0} - \frac{S(b_0 - \Delta b_i)}{S_0}}{\frac{2\Delta b}{b_0}}\,, \tag{7}$$

where $S_0 = S_0(b_0)$ is state variable value corresponding to the initial value of a design variable b_0, Δb_i is the variation of a chosen design variable and $S = S(b_0 + \Delta b_i)$ is a state variable value related with the updated value of design variable $b_0 + \Delta b_i$.

5. Numerical example

5.1. Description of numerical example

In order to conduct multiparameter sensitivity analysis, the computational model of the footbridge was divided into 285 independent areas as presented in Fig. 5a. Fifteen segments, 0.5 m long were established along the structure, named S1÷S14, while the last one, S15, located near the mid-span is 0.25 m long. Additionally, looking at the cross-sectional walls and deck, they were also divided into three sections of a length about 0.43-0.44 m (Fig. 5b). Thus the inner laminate, PET foam and outer laminate in wall and deck were divided into 15x3 = 45 areas, respectively. Furthermore, the laminate in a handrail was divided into 15 areas. As a result, 285 design variables were obtained to be classified into two types with respect to material. It was assumed that the laminate thickness is variable as it can be made of a different number of plies. On the other hand, the thickness of PET foam cannot change. However, locally, the foam may exhibit various density, therefore, various material parameters. Thus, the vector of design variables can be expressed as

$$\mathbf{b} = \{\underbrace{t_1, t_2, ..., t_i, ..., t_{195}}_{\text{laminate}}, \underbrace{E_{196}, E_{197}, ..., E_j, ..., E_{285}}_{\text{PET foam}}\}^T. \tag{8}$$

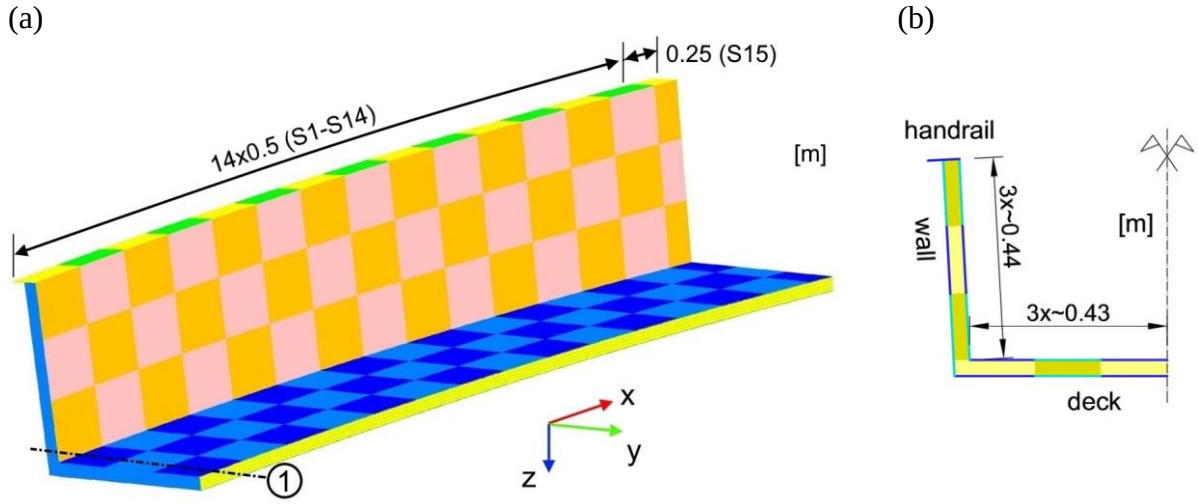

Fig. 5. The footbridge divided into 285 independent areas: (a) overall view, (b) cross-section

According to the Eurocode, both structural ULS and SLS have to be analyzed, hence, stress or strain and displacement may be considered state variables, respectively. The extreme stresses in a laminate are assumed at a relatively low level – the failure index IF cannot exceed 0.2 according to Tsai-Wu hypothesis. Thus the Serviceability Limit State becomes more significant, as a consequence, vertical displacement v_z in the middle of width and length of the structure (Fig. 3a) is assumed a state variable. However, additionally, longitudinal strain in handrail ε_{x1} and transverse strain ε_{y2} in outer laminate, both in the middle of footbridge length (Fig. 3a), were adopted as state variables as well, in order to investigate the impact of variation of design variables on their variations.

5.2. Results

The structure was divided into 285 independent sections – the wall and deck into 45 areas and the handrail into 15 areas. The elements of a design variable vector (eq. (8)) are mutually independent, varying at the level from -50% to 50% with respect to their initial values. Thus, laminate thickness ranges from $1.989 \cdot 10^{-3}$ m to $5.967 \cdot 10^{-3}$ m, the elastic modulus of PET foam ranges value from 35 MPa to 105 MPa. Hence, 285 sensitivity coefficients were computed according to eq. (7).

While the sensitivity analysis is performed, the 285-elemental vector of sensitivity coefficients is divided into 6 matrices with 3 rows and 15 columns that represent inner laminate, foam and outer laminate in wall and deck, additionally, into a single vector with 15 elements that represent laminate in a handrail. The example of the matrix including sensitivity coefficients of thickness variation of the inner laminate in the wall reads:

$$w_{w1} = \begin{bmatrix} w_{1,1} & w_{1,2} & \cdots & w_{1,15} \\ w_{2,1} & w_{2,2} & \cdots & w_{2,15} \\ w_{3,1} & w_{3,2} & \cdots & w_{3,15} \end{bmatrix}, \tag{8}$$

where rows and columns represent the height of wall and segments along the length, respectively, as presented in Fig. 5a.

The circles shown in the following figures represent central points of independent areas where the sensitivity coefficients are determined. In order to receive more precise results, the values of sensitivity coefficients are interpolated between these points with the 3-rd order polynomial, at the same time, extrapolated in the range from external points to the boundaries of wall, deck or handrail. Thus, the sensitivity areas are obtained of each structural element. Furthermore, in order to present sensitivity areas according to eq. (7) the sensitivity coefficient is divided by a relevant area shown in Fig. 5a. Hence, in the following figures, the colors represent the values of a relative sensitivity coefficient in unit $[\% / \mathrm{m}^2]$. The values marked in color have to be integrated to obtain sensitivity coefficient in unit [%], multiplying the computed coefficient by the appropriate surface. Subsequently, the computed value shows the extent the state variable varies after the design variable increase by 50% with respect to its initial value.

5.2.1. The impact of laminate thickness variation on the variation of displacement v_z

First of all, vertical displacement v_z is assumed a state variable, the laminate thickness is a design variable. The impact of laminate thickness variation on the variation of displacement v_z is shown in the form of sensitivity areas in Fig. 6-Fig. 8. The extreme sensitivity occurs in handrails (Fig. 6) and in outer laminate in the deck (Fig. 8b) near the mid-span reaching up to -8.5 %/m^2. Thus, multiplying the value by the area e.g. 1 m^2 shows that after increasing the laminate thickness in this region by 50% vertical displacement v_z decreases by 8.5 %. Moreover, in both inner and outer laminates of the wall the highest sensitivity absolute value occurs in the upper part for about 2/3 of the length. Additionally, in the inner laminate of the wall sensitivity increases in the lower part near the support. Finally, considering the deck, in both inner and outer laminates, the highest sensitivity absolute value appears around its middle width and length, reaching the mentioned value over -8.5 %/m^2.

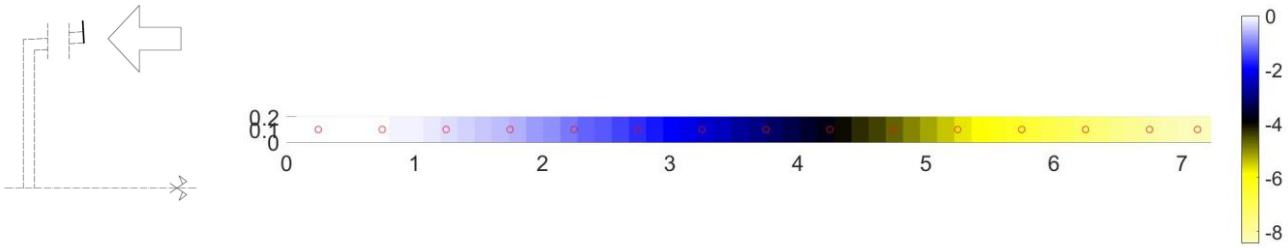

Fig. 6. The impact of laminate thickness variation on the variation of displacement – sensitivity areas [%/m^2] of the handrail

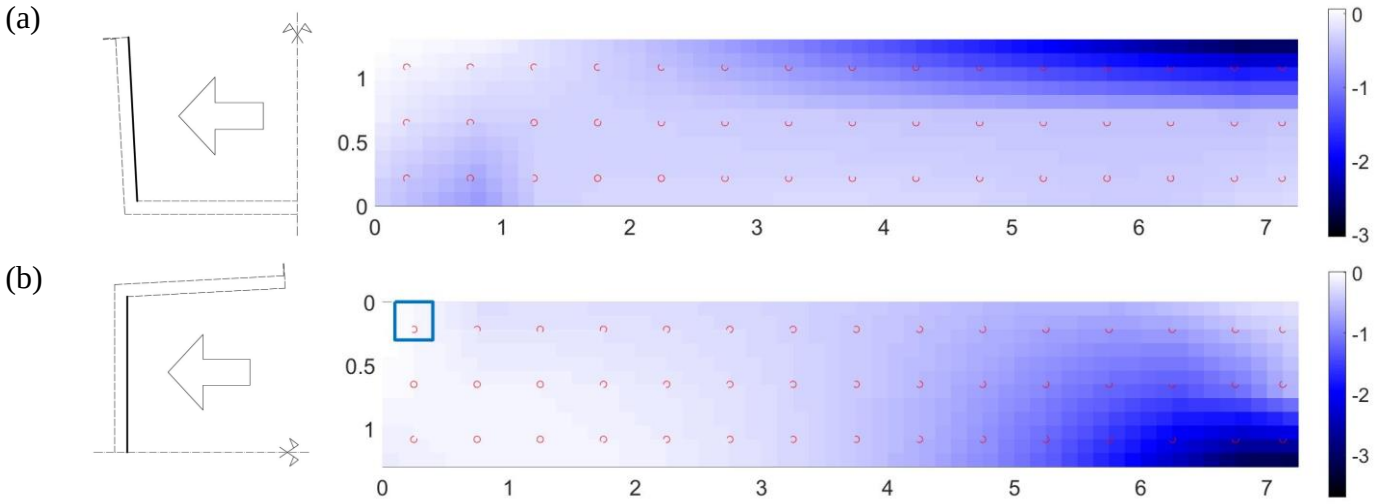

Fig. 7. The impact of laminate thickness variation on the variation of displacement – sensitivity areas [%/m^2] of the inner laminate (a) of the wall, (b) of the deck

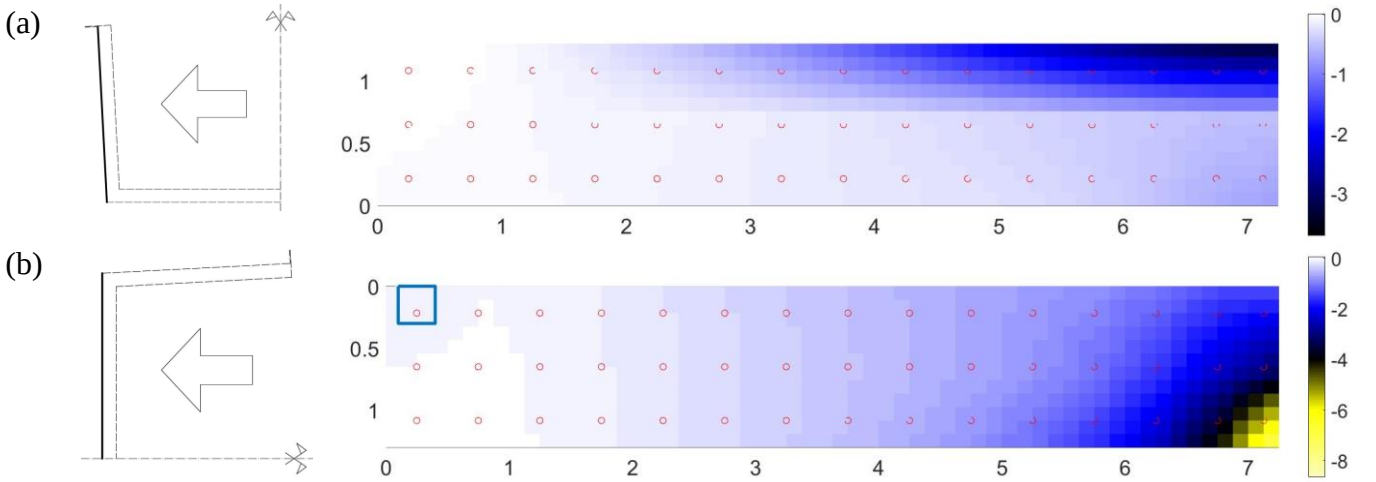

Fig. 8. The impact of laminate thickness variation on the variation of displacement – sensitivity areas [%/m^2] of the outer laminate (a) of the wall, (b) of the deck

5.2.2. The impact of PET foam stiffness modulus variation on the displacement v_z variation

Furthermore, the impact of PET foam stiffness modulus variation on variation of displacement v_z is addressed, the corresponding sensitivity areas are presented in Fig. 9. With regard to the deck, the highest absolute value of sensitivity occurs near the support zone, reaching around -8 %/m^2. Thus strengthening this area with a block of PET foam of dimensions 0.5 x 0.5 m and with the elastic modulus increased by 50% makes the vertical displacement decreased by 2%. Moreover, the sensitivity near mid-span reaches -2 %/m^2. On the other hand,

nearly 1/4 of the deck surface shows sensitivity equal to 0 %/m^2 which means, that in this area the foam with decreased stiffness can be inserted without any negative impact on displacement. Additionally, considering the wall, minimum sensitivity occurs in the bottom of the wall around support and in the top around mid-span.

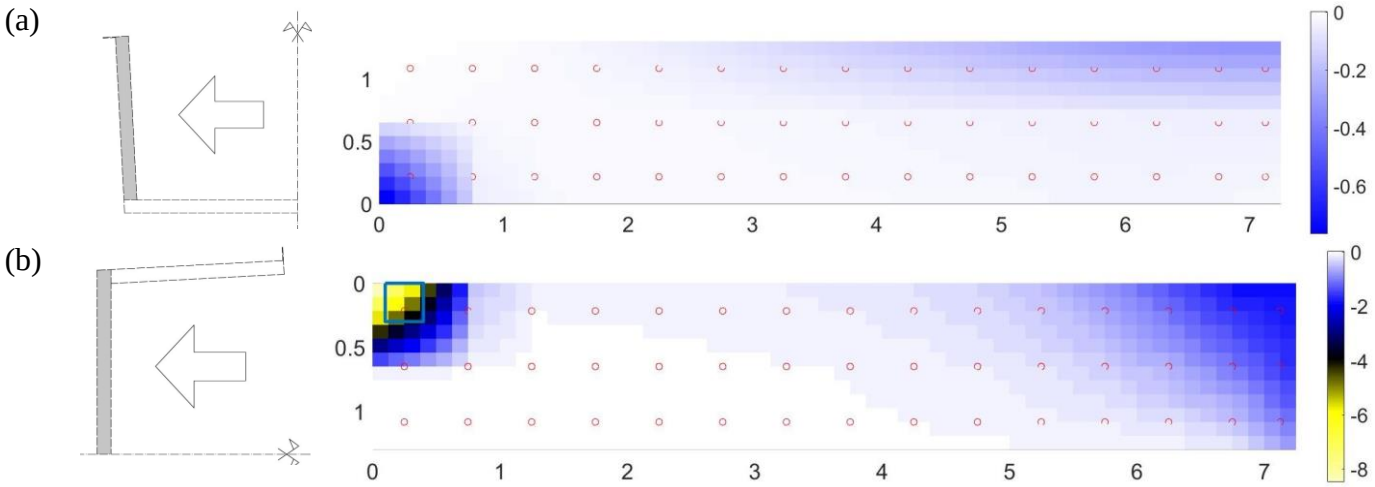

Fig. 9. The impact of PET foam stiffness modulus variation on the variation of displacement – sensitivity areas [%/m^2] of PET foam: (a) of the wall, (b) of the deck

5.2.3. The impact of laminate thickness variation on the variation of longitudinal strain ε_{x1}

Subsequently, the longitudinal strain is presented in a handrail in the mid-span of the footbridge ε_{x1} (Fig. 3a) assumed state variable and the thickness of laminate as a design variable. Sensitivity areas, showing impact of laminate thickness variation on the variation of strain, are presented in Fig. 10-Fig. 12. The results are more complex here. The sensitivity coefficients are both negative and positive, which means that the increased laminate thickness may cause a decrease or increase of the strain. Considering the handrail (Fig. 10), sensitivity is nearly zero from the support along the length of about 5 m, after which from 5 m it increases up to 10 %/m^2, to finally fall to -10 %/m^2 near the mid-span. The related results occur in the top of the inner (Fig. 11a) and outer (Fig. 11a) laminates of the wall. However, below, about halfway down, the sensitivity coefficients take mainly negative value, to become positive again in the bottom of the walls. On the other hand, in the deck, the minimum sensitivity value occurs

in the outer laminate under the wall in the mid-span equal -5.5 %/m^2, while the maximum value appears in the inner laminate in the middle of the width reaching 1 %/m^2.

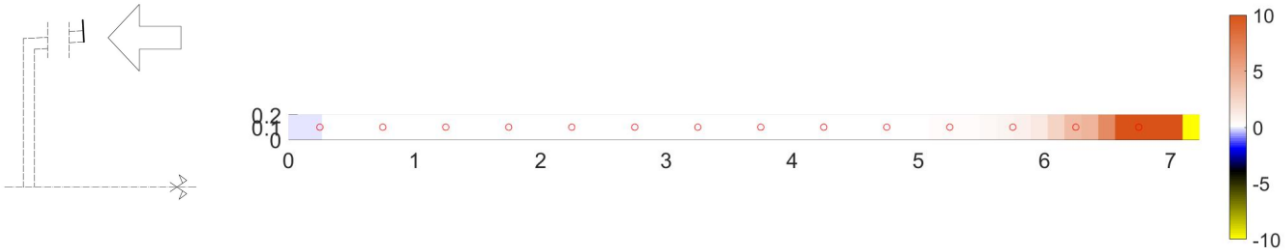

Fig. 10. The impact of laminate thickness variation on the variation of longitudinal strain – sensitivity areas [%/m^2] of the handrail

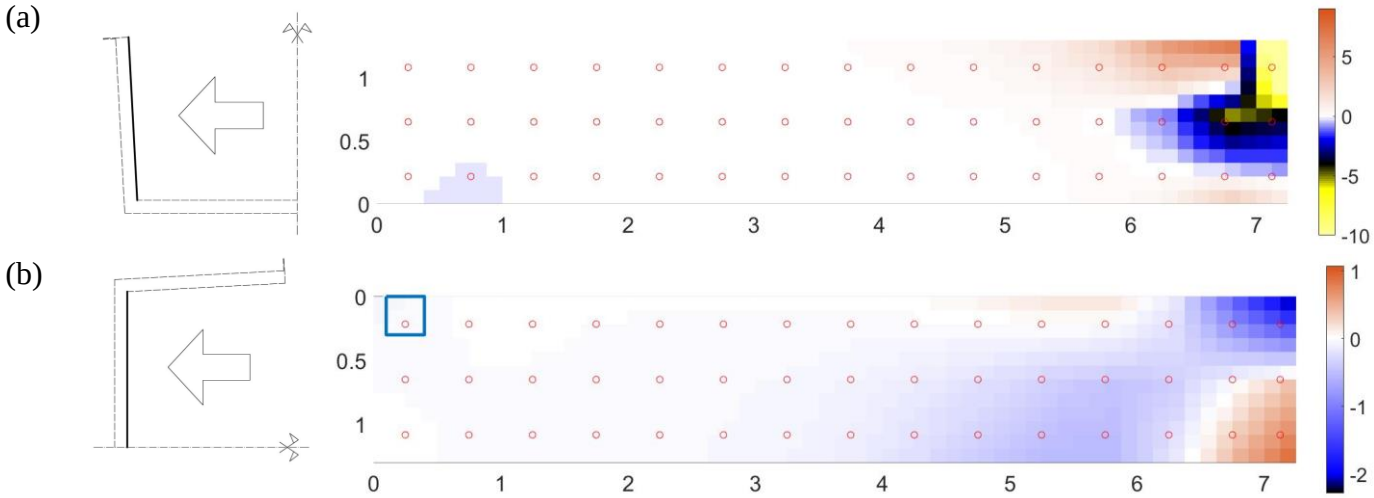

Fig. 11. The impact of laminate thickness variation on the variation of longitudinal strain – sensitivity areas [%/m^2] of the inner laminate (a) of the wall, (b) of the deck

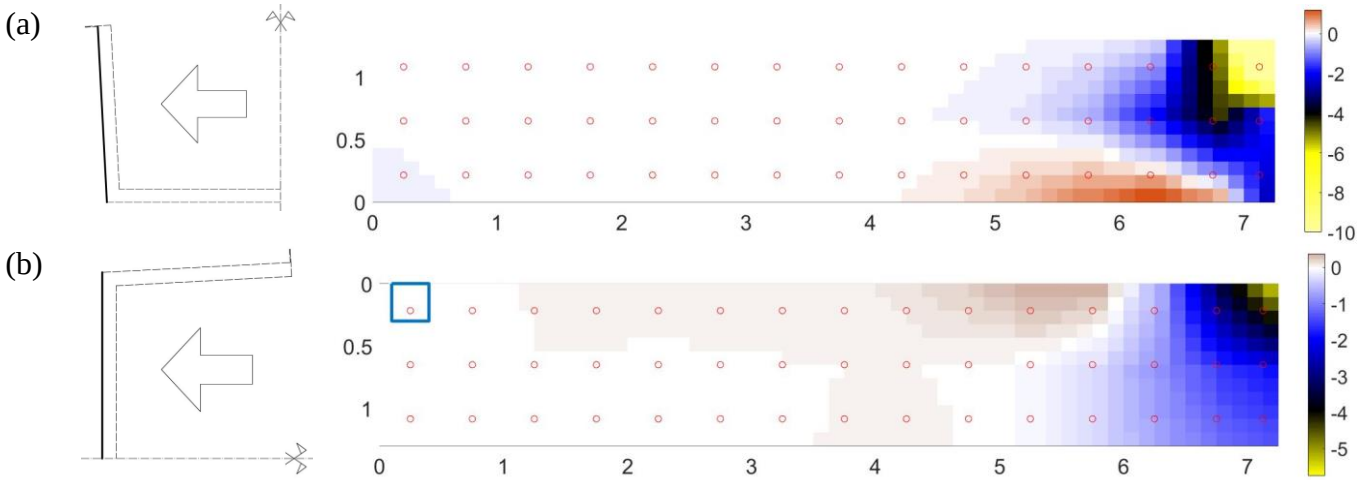

Fig. 12. The impact of laminate thickness variation on the variation of longitudinal strain – sensitivity areas [%/m^2] of the outer laminate (a) of the wall, (b) of the deck

5.2.4. The impact of foam stiffness modulus variation on the variation of longitudinal strain ε_{x1}

Afterwards, the impact of variation of PET foam stiffness modulus on variation of longitudinal strain ε_{x1} is computed and presented in the form of sensitivity areas in Fig. 13. Considering the wall, the extreme value occurs in its top near the mid-span of the footbridge reaching -5.5 %/m^2. Except that area, the sensitivity value is around 0 %/m^2, which means that neither increasing nor decreasing the stiffness modulus of PET foam affects the change in strain. In the case of deck, the only area of positive sensitivity coefficient is the support zone. The sensitivity values are displayed in the form of a surface area of 0.5 x 0.5 m dimensions, taking values up to -2.5 %/m^2.

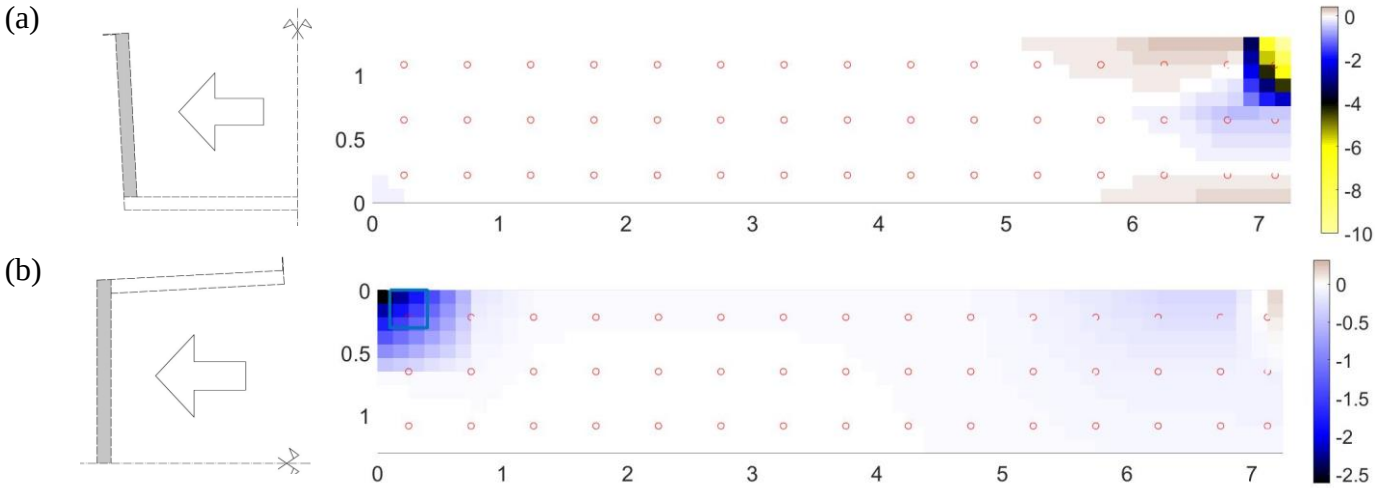

Fig. 13. The impact of PET foam stiffness modulus variation on the variation of longitudinal strain – sensitivity areas [%/m^2] of PET foam (a) of the wall, (b) of the deck

5.2.5. The impact of laminate thickness variation on the variation of transverse strain ε_{y2}

Finally, the transverse strain in the outer laminate in the middle of the footbridge width and length ε_{y2} (Fig. 3a) are assumed state variable, the thickness of laminate is a design variable. Sensitivity areas are shown in Fig. 14-Fig. 16. Sensitivity coefficients may take both negative and positive values, like before. The extreme absolute value of sensitivity coefficient exceeds 10 %/m^2, mainly in the inner and outer laminates of the deck in the mid-span of the footbridge.

However, at the point in the middle of structural length and width, in the inner laminate, the sensitivity coefficient is positive while in the outer laminate it is negative. Thus, increasing thickness of inner laminate in this area causes significant increase of the considered strain. On the other hand, increasing thickness of the outer laminate leads to high decrease of a state variable. Furthermore, the presented sensitivity areas exhibit high variability. The maximum and minimum values of sensitivity coefficients occur in close proximity. The extreme values appear at a distance of about 1 m.

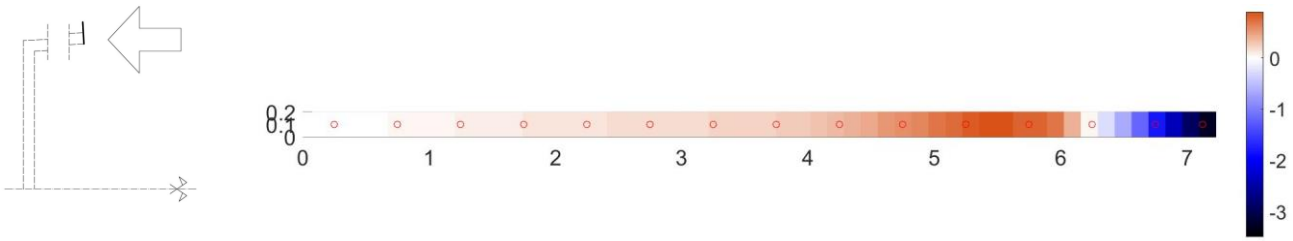

Fig. 14. The impact of laminate thickness variation on the variation of transverse strain – sensitivity areas [%/m^2] of the handrail

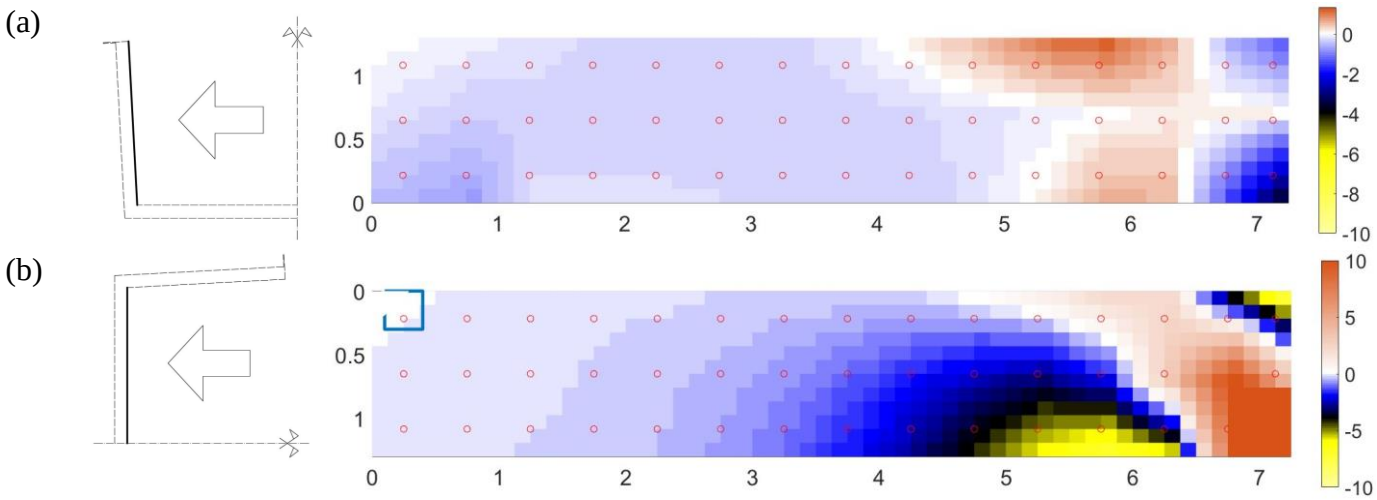

Fig. 15. The impact of laminate thickness variation on the variation of transverse strain – sensitivity areas [%/m^2] of the inner laminate: (a) of the wall, (b) of the deck

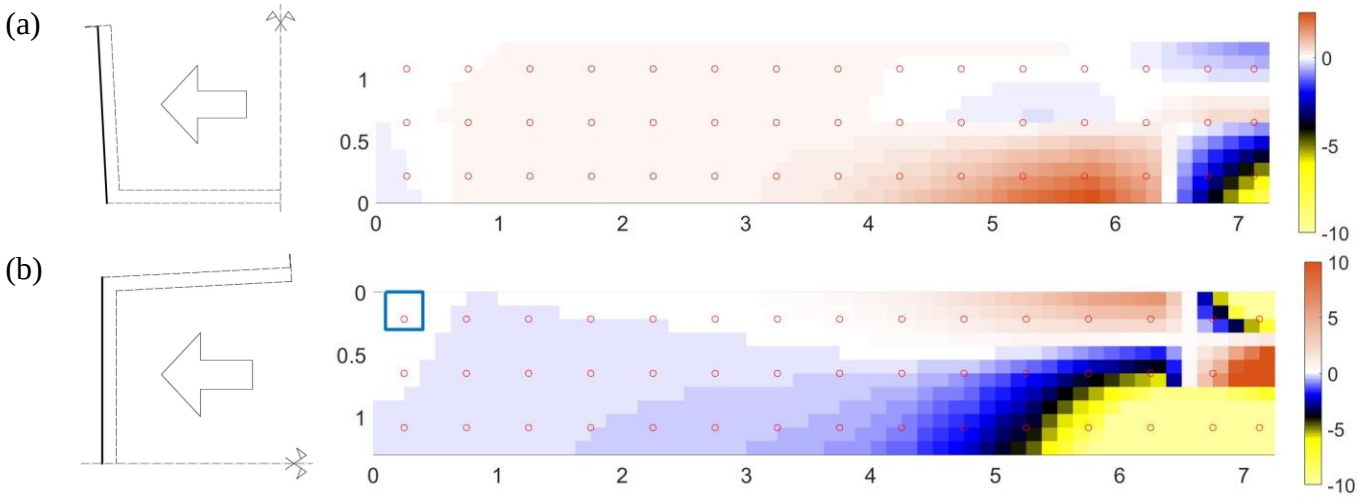

Fig. 16. The impact of laminate thickness variation on the variation of transverse strain – sensitivity areas [%/m^2] of the outer laminate: (a) of the wall, (b) of the deck

5.2.6. The impact of foam stiffness modulus variation on the variation of transverse strain ε_{y2}

In addition, the influence of PET foam stiffness modulus variation on the variation of transverse strain ε_{y2} are presented in the form of sensitivity areas in Fig. 17. The sensitivity coefficients in the wall are relatively low, they reach extreme values of about -0.25 %/m^2. However, in the deck, the value becomes significant, it exceeds 10 %/m^2 in the mid-span of the footbridge. Thus, increasing the stiffness modulus in this areas make the transverse strain in the outer laminate increase. On the other hand, from 0 m to 6.5 m of the length the sensitivity coefficients are negative, taking values up to -5 %/m^2

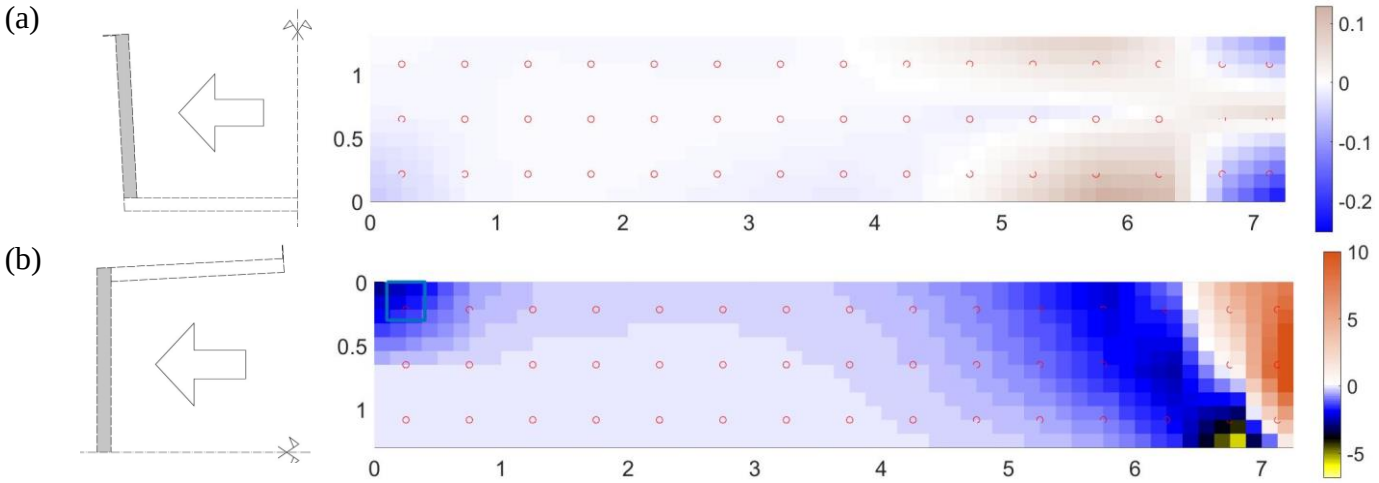

Fig. 17. The impact of PET foam stiffness modulus variation on the variation of transverse strain – sensitivity areas [%/m^2] of PET foam: (a) of the wall, (b) of the deck

6. Conclusions

The paper focuses on multiparameter semi-analytical sensitivity analysis of U-shaped composite footbridge of a sandwich structure. The sensitivity vector that consists of sensitivity coefficients is computed by FEM and expressed in a matrix form, next represented graphically in the form of sensitivity areas. The conducted sensitivity analysis shows the regions to be strengthened in order to minimize vertical displacement, longitudinal strain in handrail and transverse strain deck in selected points, and the sections where the parameters can be reduced without the increment of state variables.

Considering vertical displacement in the middle of the footbridge length and width, all sensitivity coefficients are negative. Therefore, increasing laminate thickness or elastic modulus of PET foam, a reduced displacement is obtained. Moreover, sensitivity areas indicate the regions with the highest impact of variation of the mentioned parameters on variation of considered displacement – the laminate in the deck in the mid-span of the footbridge, the top of wall, and PET foam near support zone.

In terms of vertical displacement sensitivity coefficients are always negative, thus due to the considered longitudinal and transverse strain sensitivity coefficients take both negative and positive values. Thus increasing thickness of laminates or stiffness modulus of PET foam results in a decrease or increase of strain depending on the area.

The presented sensitivity analysis, linked identification and optimization, forms divisions of theory of design. Sensitivity analysis shows similarities with optimization process, the latter, in order to find optimal solution, defines the objective function with set constrains determined by the design variables. The results are the final values of design variables. However, sensitivity analysis studies the relations between variations of design variables and state variables, providing more information for structural designer on the areas which affect chosen state variables in greater, lower or none extent. Hence, the obtained sensitivity analysis results may

support structural design process and the development of designed or existing structures to bring a more competitive product in the global market.

Finally, the paper proves sensitivity analysis as a very helpful tool. Along with optimization, it can be effectively applied in the process of identifying parameters defining the numerical model. The final decision is always the designer's work, but advanced, comprehensive methods provide him with the tools to complete the task successfully.

Acknowledgments

The study was supported by the National Centre for Research and Development, Poland, grant no PBS1/B2/6/2013.

References

[1] Haug E.J., Choi K.K. & Komkov V. (1986) Design Sensitivity Analysis of Structural Systems. Academic Press Fl, Orlando.

[2] F.van Keulen, R.T.Haftka, N.H.Kim (2005) Review of options for structural design sensitivity analysis. Part 1: Linear systems, Computer Methods in Applied Mechanics and Engineering, Volume 194, Issues 30–33, Pages 3213-3243, doi: 10.1016/j.cma.2005.02.002

[3] Haug E.J., Arora J.S., Applied Optimal Design, New York-Chichester-Brisbane-Toronto, John Wiley and Sons, 1979.

[4] Nocedal J., Wright S.J., Numerical Optimization, Springer, 1999

[5] Mazurkiewicz Ł., Małachowski J., Baranowski P. (2015) Optimization of protective panel for critical supporting elements, Composite Structures, 134 (2015) 493–505, doi: 10.1016/j.compstruct.2015.08.069

[6] Mazurkiewicz Ł., Małachowski J., Damaziak K., Tomaszewski M. (2018): Evaluation of the response of fibre reinforced composite repair of steel pipeline subjected to puncture from excavator tooth, Composite Structures, 202 (2018) 1126–1135, doi: 10.1016/j.compstruct.2018.05.065

[7] Akihiro Takezawa, Mitsuru Kitamura (2013) Sensitivity analysis and optimization of vibration modes in continuum systems, Journal of Sound and Vibration, Volume 332, Issue 6, Pages 1553-1566, doi: 10.1016/j.jsv.2012.11.015

[8] V.Kumar, S.-J.Lee, M.D.German (1989) Finite element design sensitivity analysis and its integration with numerical optimization techniques for structural design, Computers & Structures, Volume 32, Issues 3–4, Pages 883-897, doi: 10.1016/0045-7949(89)90372-6

[9] Qimao Liu, Juha Paavola (2018) General analytical sensitivity analysis of composite laminated plates and shells for classical and first-order shear deformation theories, Composite Structures, Volume 183, Pages 21-34, doi: 10.1016/j.compstruct.2016.11.052

[10] Xiaochen Hang, Weihua Su, Qingguo Fei, Dong Jiang (2020) Analytical sensitivity analysis of flexible aircraft with the unsteady vortex-lattice aerodynamic theory, Aerospace Science and Technology, Volume 99, 105612, doi: 10.1016/j.ast.2019.105612

[11] Kaichao Zhang, Zhenzhou Lu, Danqing Wu, Yongli Zhang (2017) Analytical variance based global sensitivity analysis for models with correlated variables, Applied Mathematical Modelling, Volume 45, Pages 748-767, doi: 10.1016/j.apm.2016.12.036

[12] Yueying Zhu, Qiuping Alexandre Wang, Wei Li, Xu Cai (2017) An analytic method for sensitivity analysis of complex systems, Physica A: Statistical Mechanics and its Applications, Volume 469, Pages 52-59, doi: 10.1016/j.physa.2016.11.059

[13] Qimao Liu (2015) Analytical sensitivity analysis of frequencies and modes for composite laminated structures, International Journal of Mechanical Sciences, Volume 90, Pages 258-277, doi: 10.1016/j.ijmecsci.2014.11.018

[14] Félix Nieto, Santiago Hernández, José Á.Jurado Alejandro Mosquera (2011) Analytical approach to sensitivity analysis of flutter speed in bridges considering variable deck mass, Advances in Engineering Software, Volume 42, Issue 4, Pages 117-129, doi: 10.1016/j.advengsoft.2010.12.003

[15] Cheng G, Olhoff N. (1993) Rigid body motion test against error in semi-analytical sensitivity analysis, Computers & Structures, Vol. 46, No. 3, pp. 515-527, doi: 10.1016/0045-7949(93)90221-X

[16] Bruno Barthelemy, Choon T.Chon, Raphael T.Haftka (1988) Accuracy problems associted with semi-analytical derivatives of static response, Finite Elements in Analysis and Design, Volume 4, Issue 3, Pages 249-265, doi: 10.1016/0168-874X(88)90011-X

[17] Kai-Uwe Bletzinger, Matthias Firl, Fernass Daoud (2008) Approximation of derivatives in semi-analytical structural optimization, Computers & Structures, Volume 86, Issues 13–14, Pages 1404-1416, doi: 10.1016/j.compstruc.2007.04.014

[18] H.de Boer, F.van Keulen (2000) Refined semi-analytical design sensitivities, International Journal of Solids and Structures, Volume 37, Issues 46–47, Pages 6961-6980, doi: 10.1016/S0020-7683(99)00322-4

[19] J. Kiendl, R. Schmidt, R. Wüchner, K.-U. Bletzinger (2014) Isogeometric shape optimization of shells using semi-analytical sensitivity analysis and sensitivity weighting, Computer Methods in Applied Mechanics and Engineering, Volume 274, Pages 148-167, doi: 10.1016/j.cma.2014.02.001

[20] Wenjia Wang, Peter M.Clausen, Kai-Uwe Bletzinger (2015) Improved semi-analytical sensitivity analysis using a secant stiffness matrix for geometric nonlinear shape optimization, Computers & Structures, Volume 146, Pages 143-151, doi: 10.1016/j.compstruc.2014.08.008

[21] Robert Sonnenschein, Katarina Gajdosova, Ivan Holly (2016) FRP Composites and their Using in the Construction of Bridges, Procedia Engineering, Volume 161, Pages 477-482, doi: 10.1016/j.proeng.2016.08.665

[22] Keller, T. (2002). Overview of Fibre-Reinforced Polymers in Bridge Construction. Structural Engineering International, 12(2), 66–70. doi:10.2749/101686602777965595.

[23] M.Klasztorny, A.Bondyra, P.Szurgott, D.Nycz (2012) Numerical modelling of GFRP laminates with MSC.Marc system and experimental validation, Computational Materials Science, Volume 64, Pages 151-156, doi: 10.1016/j.commatsci.2012.05.024

[24] Asby M., Jones D (1999) Engineering Materials 1, Butterwoth-Heinemann, England

[25] Harris B. (1999) Engineering Composite Materials, The Institute of Materials, London

[26] Tomasz Siwowski, Maciej Kulpa, Mateusz Rajchel, Pawel Poneta (2018) Design, manufacturing and structural testing of all-composite FRP bridge girder, Composite Structures, Volume 206, Pages 814-827, doi: 10.1016/j.compstruct.2018.08.048

[27] Tomasz Siwowski, Mateusz Rajchel, Maciej Kulpa (2019) Design and field evaluation of a hybrid FRP composite – Lightweight concrete road bridge, Composite Structures, Volume 230, 111504, doi: 10.1016/j.compstruct.2019.111504

[28] Tomasz Siwowski, Mateusz Rajchel (2019) Structural performance of a hybrid FRP composite – lightweight concrete bridge girder, Composites Part B: Engineering, Volume 174, 107055, doi: 10.1016/j.compositesb.2019.107055

[29] Yaqiang Yang, Mohamed F.M.Fahmy, Sujun Guan, Zhihong Pan, Yang Zhan, Tidong Zhao (2020) Properties and applications of FRP cable on long-span cable-supported

bridges: A review, Composites Part B: Engineering, Volume 190, 107934, doi: 10.1016/j.compositesb.2020.107934

[30] Yaqiang Yang, Xin Wang, Zhishen Wu (2020) Long-span cable-stayed bridge with hybrid arrangement of FRP cables, Composite Structures, Volume 237, 111966, doi: 10.1016/j.compstruct.2020.111966

[31] Julio F.Davalos, An Chen, Bin Zou (2012) Performance of a scaled FRP deck-on-steel girder bridge model with partial degree of composite action, Engineering Structures, Volume 40, Pages 51-63, doi: 10.1016/j.engstruct.2012.02.020

[32] Kulpa M. & Siwowski T. (2018). Stiffness and strength evaluation of a novel FRP sandwich panel for bridge redecking. Composite Part B, 167, 207-220. doi: 10.1016/j.compositesb.2018.12.004

[33] Chróścielewski, J., Miśkiewicz, M., Pyrzowski, Ł. & Wilde, K. (2017). Composite GFRP U-Shaped Footbridge. Polish Maritime Research, 24(s1). doi:10.1515/pomr-2017-0017

[34] Yeou-Fong Li, Sainey Badjie, Walter W.Chen, Yu-Tsung Chiu (2014) Case study of first all-GFRP pedestrian bridge in Taiwan, Case Studies in Construction Materials, Volume 1, Pages 83-95, doi: 10.1016/j.cscm.2014.05.001

[35] Xiaojun Wei, Hua-Ping Wan, Justin Russell, Stana Živanović, Xuhui He (2019) Influence of mechanical uncertainties on dynamic responses of a full-scale all-FRP footbridge, Composite Structures, Volume 223, 110964, doi: 10.1016/j.compstruct.2019.110964

[36] Marian Klasztorny, Kamil Pawel Zajac, Daniel Bronislaw Nycz (2020) GFRP composite footbridge series with multi-box cross section – Part 1: Design methodology, conceptual design and global detailed design, Composite Structures, Volume 238, 111965, doi: 10.1016/j.compstruct.2020.111965

[37] M. Klasztorny, D.B. Nycz, K.P. Zając (2018) Advanced design calculations of composite box footbridge, Composites Theory and Practice, 18 (1) pp. 37-44

[38] Saima Ali, David Thambiratnam, Xuemei Liu, Sabrina Fawzia (2020) Performance evaluation of innovative composite pedestrian bridge, Structures, Volume 26, Pages 845-858, doi: 10.1016/j.istruc.2020.05.010

[39] Chróścielewski J, Klasztorny M, Romanowski R, Barnat W, Małachowski J, Derewońko A, et al. (2015) Badania eksperymentalne identyfikacyjne kompozytu. Raport z realizacji podzadania 5.1 WAT (internal report), Warsaw (in Polish)

[40] Pyrzowski Ł (2018) Testing Contraction and Thermal Expansion Coefficient of Construction and Moulding Polymer Composites, Polish Maritime Research, vol. 25, no. s1, pp. 151–158, doi: 10.2478/pomr-2018-0036

[41] Pyrzowski, Ł., Sobczyk, B., Witkowski, W., & Chróścielewski, J. (2016). Three-point bending test of sandwich beams supporting the GFRP footbridge design process—validation. Advances in Mechanics: Theoretical, Computational and Interdisciplinary Issues, 489–492. doi:10.1201/b20057-104.

[42] Chróścielewski J., Ferenc T., Mikulski T., Miśkiewicz M., Pyrzowski Ł. (2019) Numerical modeling and experimental validation of full-scale segment to support design of novel GFRP footbridge, Composite Structures. Vol. 213, pp.299-307, doi: 10.1016/j.compstruct.2019.01.089

[43] Miśkiewicz M., Daszkiewicz K., Ferenc T., Witkowski W., Chróścielewski J. (2016) Experimental tests and numerical simulations of full scale composite sandwich segment of a foot- and cycle- bridge, Advances in Mechanics: Theoretical, Computational and Interdisciplinary Issues, 401-404, 2016, Taylor & Francis Group

[44] Ferenc T., Mikulski T. (2020) Validation process for computational model of full-scale segment for design of composite footbridge, Polish Maritime Research, No 2(106), Vol 27, pp. 158-167, doi: 10.2478/pomr-2020-0037

[45] Wiczenbach T., Ferenc T., Pyrzowski Ł., Chróścielewski J. (2019): Dynamic Tests of Composite Footbridge Segment–Experimental and Numerical Studies, MATEC Web of Conferences, 285, 00021, DOI: 10.1051/matecconf/201928500021

[46] Chróścielewski J., Miśkiewicz M., Pyrzowski Ł., Sobczyk B. & Wilde K. (2017) A novel sandwich footbridge - Practical application of laminated composites in bridge design and in situ measurements of static response, Composites Part B 126, 153-161

[47] Chróścielewski J., Miśkiewicz M., Pyrzowski Ł., Rucka M., Sobczyk B. & Wilde K (2018) Modal properties identification of a novel sandwich footbridge – Comparison of measured dynamic response and FEA, Composites Part B 151, 245-255

[48] Ferenc T., Mikulski T. (2020) Parametric Optimization of Sandwich Composite Footbridge with U-shaped Cross-Section, Composite Structures, 246, 112406, doi: 10.1016/j.compstruct.2020.112406

[49] Ferenc T., Pyrzowski Ł., Chróścielewski J. & Mikulski T. (2018) Sensitivity analysis in designing process of sandwich U-shaped composite footbridge, Shell Structures: Theory and Applications. - Vol. 4, ed. W. Pietraszkiewicz, W. Witkowski, Leiden: CRC Press/Balkema, 413-416, doi:10.1201/9781315166605-94

[50] Chróścielewski J, Klasztorny M, Nycz D, Sobczyk B. (2014) Load capacity and serviceability conditions or footbridges made of fibre-reinforced polymer laminates. Roads Bridges;13,189-202. http://dx.doi.org/10.7409/rabdim.014.013

[51] Tsai S. W. & Wu E. M. (1971) A general theory of strength for anisotropic materials, J. Comp. Mater. 5 (1)

[52] Tsai S. W &, Hahn H. T. (1980) Introduction to composite materials, Technomic Publishing Co., Lancaster, USA

[53] Chen Fu, Xi Wang (2020) Micro-mechanical analysis of matrix crack-induced delamination in cross-ply laminates in tension, Composite Structures, Volume 243, 112202, doi: 10.1016/j.compstruct.2020.112202

[54] PN-S-10052-1982 Bridges, Steel Structures, Design (in Polish)

[55] Serge Abrate, Marco Di Sciuva (2017) Equivalent single layer theories for composite and sandwich structures: A review, Composite Structures, Volume 179, Pages 482-494, doi: 10.1016/j.compstruct.2017.07.090

[56] A.Ahmed, L.J.Sluys (2013) A three-dimensional progressive failure model for laminated composite plates subjected to transverse loading, Engineering Fracture Mechanics, Volume 114, Pages 69-91, doi: 10.1016/j.engfracmech.2013.10.004

[57] Chien H. Thai, Magd Abdel Wahab, Hung Nguyen-Xuan (2018) A layerwise C0-type higher order shear deformation theory for laminated composite and sandwich plates, Comptes Rendus Mécanique, Volume 346, Issue 1, Pages 57-76, doi: 10.1016/j.crme.2017.11.001

[58] J.E.Semedo Garção, C.M.Mota Soares, C.A.Mota Soares, J.N.Reddy (2004) Analysis of laminated adaptive plate structures using layerwise finite element models, Computers & Structures, Volume 82, Issues 23–26, Pages 1939-1959, doi: 10.1016/j.compstruc.2003.10.024